NJC

PAPER

View Article Online
View Journal | View Issue

Cite this: *New J. Chem.*, 2014, **38**, 1199

Gold(III) complexes of 5-methyl-5-(pyridyl)-2,4-imidazolidenedione: synthesis, physicochemical, theoretical, antibacterial, and cytotoxicity investigation†

Seyyed Javad Sabounchei,*[a] Parisa Shahriary,[a] Sadegh Salehzadeh,[a] Yasin Gholiee,[a] Davood Nematollahi,[a] Abdolkarim Chehregani[b] and Amene Amani[a]

Received (in Victoria, Australia) 2nd September 2013,
Accepted 28th November 2013

DOI: 10.1039/c3nj01042b

www.rsc.org/njc

This work reports the synthesis and characterization of cytotoxic gold(III) complexes of a series of 5-methyl-5-(pyridyl)-2,4-imidazolidenedione ligands. Based on the elemental analysis and inductively coupled plasma-mass spectrometry (ICP-MS), the complexes have the general formula Au**L1**Cl_2 (**1**), [Au(**L2**)$_2Cl_2$][$AuCl_4$] (**2**), and [Au(**L3**)$_2Cl_2$][$AuCl_4$] (**3**) (**L1**, **L2**, and **L3** = 5-methyl-5-(2,3, and 4-pyridyl)-2,4-imidazolidenedione, respectively). All the compounds were studied by means of IR, ^{1}H, ^{13}C NMR spectral analyses, molar conductivity, cyclic voltammetry, and DFT methods. The studies showed the complexes have square planar geometry, common for d^8 complexes, with the ligand molecule coordinated in an *N*-coordination bidentate (**1**) and monodentate (**2** and **3**) fashion to the metal center. DFT studies on different geometrical isomers suggested that in both the gas and solution phases, the *trans* isomers for **2** and **3** are more stable than the *cis* ones. The antibacterial activity and *in vitro* cytotoxicity of these compounds, as respectively assessed in six bacterial strains and two human tumor cell lines, have been investigated. The results showed the title complexes have the capacity to inhibit the metabolic growth of the investigated bacteria and tumor cells to different extents. The cytotoxicity profiles of the complexes against MCF-7 tumor cell lines are comparable to that of cisplatin (*cis*-diamminedichloroplatinum(II), DDP).

Introduction

Over the past few years, much interest has focused on gold(III) complexes. Au(III) complexes are square-planar d^8, isoelectronic and isostructural to platinum(II) complexes, and therefore they appear to be very good candidates for anticancer investigations.[1–5]

Though a number of interesting Au(III) targets have been investigated,[6,7] the biological utility of such agents continues to be questioned. This may be due, in part, to the reductive potential and poor solubility of common Au(III) coordination complexes under physiological conditions. Many groups are providing insight into complexes of Au(III) that may possess significant anticancer activity. These range from simple Au(III) coordination complexes,[4,8–17] Au(III) complexes containing bioligands,[18–31] and organometallic Au(III) species.[21,32–41] However, compared to the corresponding Pt(II) complexes, ligand substitution reactions of gold(III) complexes[42–45] have not been extensively studied because of their poor kinetic and redox stabilities, and there is a tendency for the reduction of Au(III) to Au(I) and disproportionation to colloidal Au(0).

A noteworthy approach in the design of cisplatin analogues is the use of physiologically active compounds as ligands. By replacing the labile chloride ligands with other leaving groups or by substituting amine ligands with cyclic or acyclic alkylamines, a number of other drugs have been developed. Recent studies have demonstrated that simple bidentate or polydentate ligands containing nitrogen donor atoms may offer sufficient redox stabilization to produce viable Au(III) anticancer drug targets under physiological conditions.[11] Therefore, various hydantoins

[a] *Faculty of Chemistry, Bu-Ali Sina University, Hamedan 65174, Iran. E-mail: jsabounchei@yahoo.co.uk; Fax: +98 8118 380709; Tel: +98 9183 139021*
[b] *Faculty of Science, Department of Biology, Bu-Ali Sina University, Hamedan 65174, Iran*

† Electronic supplementary information (ESI) available: ^{1}H NMR, ^{13}C NMR, IR, and ATR-IR spectra of **1** (Fig. S1–S4), ^{1}H NMR, ^{13}C NMR, IR, and ATR-IR spectra of **2** (Fig. S5–S8), ^{1}H NMR, ^{13}C NMR, IR, and ATR-IR spectra of **3** (Fig. S9–S12), solution IR spectra (Fig. S13–S17), optimized structures of two possible conformers for **L2** at the BP86/TZVP level of theory (Fig. S18), optimized structures of all possible conformers for **2** at the BP86/TZVP level of theory (Fig. S19), optimized structures of all possible conformers for **3** at the BP86/TZVP level of theory (Fig. S20), correlations between the theoretical and corresponding experimental values of ^{1}H (the left) and ^{13}C (the right) chemical shifts (δ, ppm) for **L2**, **L3**, **2**, and **3** (Fig. S21), selected bond lengths (Å) and angles (°) for **L1** and **1** (Table S1), **L2** and **2** (Table S2), and **L3** and **3** (Table S3), electronic energies (Hartree) of all possible isomers and conformers for **L2**, **2** and **3** at the BP86/TZVP level (Table S4), Cartesian coordinate representation of the optimized molecular structures of **L1–L3** and the corresponding Au(III) complexes at the BP86/TZVP level of theory. See DOI: 10.1039/c3nj01042b

and spirohydantoins can be used as carrier ligands because they are both biologically active[46] nitrogen donors. In these derivatives, strong evidence is available which indicates the crucial effect of the nature of C-5 substituents on the pharmacological action.[47] We devoted this study to the chemical modification of structures similar to cisplatin and obtained new complexes in an attempt to illuminate the anticancer potential of these compounds.

This study represents the synthesis, physicochemical evaluation, theoretical studies, and pharmacological investigation of Au(III) complexes with 5-methyl-5-pyridylhydantoins. Unfortunately, all our attempts to obtain single crystals from the newly synthesized complexes have failed. For this reason, various spectroscopic methods and DFT studies were used to elucidate their structures.

Results and discussion

Room temperature reactions of $H[AuCl_4]\cdot xH_2O$ with **L1–L3** (1 : 1 M ratio) in aqueous ethanol solution gave complexes **1–3** (Scheme 1). On the basis of the data from the elemental analysis and ICP-MS, the following formulae can be derived for the new complexes: Au**L1**Cl_2 (**1**), $[Au(\mathbf{L2})_2Cl_2][AuCl_4]$ (**2**), and $[Au(\mathbf{L3})_2Cl_2][AuCl_4]$ (**3**). Binuclear complexes **2** and **3** have $[AuCl_4]^-$ as a counter-ion,[48,49] see Scheme 1. The compounds were characterized on the basis of the following studies.

Molar conductivity studies

The molar conductance values of 10^{-3} M solutions of complexes **1–3** were measured in DMSO. The low conductance value for complex **1** (11.70 Ω^{-1} cm^2 mol^{-1}) suggested that the replacement of two chloride ligands by one **L1** had occurred to give a neutral and non-electrolytic complex,[50] where **L1** acts as a deprotonated *N*,*N*-bidentate ligand.[51] In complexes **2** and **3**, the molar conductivity values, 79.12 and 43.45 Ω^{-1} cm^2 mol^{-1}, respectively, are in the range of 1 : 1 electrolytes in this solvent.[50] This may be taken as evidence for the presence of $[AuCl_4]^-$ as a counter-ion, indicating the electrolytic nature of these complexes.

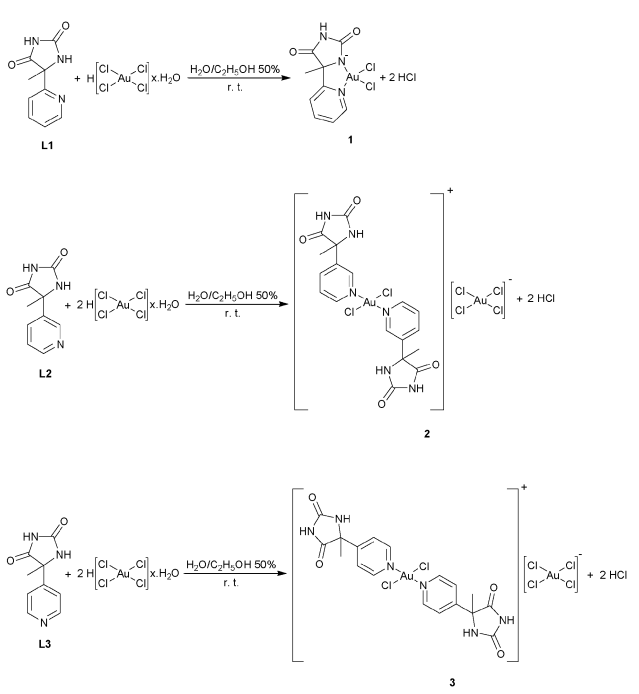

Scheme 1 Synthesis of complexes **1–3**.

Electrochemical studies

Cyclic voltammetry was used to elucidate the suggested structures for complexes **1–3**. CV curves of the all compounds at a 100 mV s^{-1} scan rate in DMSO solutions (1.0 mM) are given in Fig. 1. The reduction of Au(III) → Au(I) was observed for the Au(III) complexes and the reduction of Au(I) → Au(0) for most of the Au(I) complexes.[52] As can be seen in Fig. 1, curve a, **1** shows one irreversible cathodic peak, C_1, appearing at −0.02 V, corresponding to the two electron reduction of Au(III) to Au(I). Under these conditions, the cyclic voltammogram of **2** shows one quasi-reversible reduction process (C_2 and A_2) at 0.1 and 0.58 V, respectively, and one irreversible reduction peak (C_3) at −0.12 V *vs.* Ag/Ag$^+$ (Fig. 1, curve b). The first quasi-reversible reduction peak (C_2) is assigned to the two electron reduction of Au(III) in the $[Au(\mathbf{L2})_2Cl_2]^+$ cation, whereas the second, more intense peak C_3, is related to the two electron reduction of Au(III) to Au(I) in the counter ion, $AuCl_4^- + 2e^- \rightarrow AuCl_2^- + 2Cl^-$.[52] In this cyclic voltammogram, the anodic peak A_2 is related to the oxidation of $[Au(\mathbf{L2})_2Cl_2]^+$ to $[Au(\mathbf{L2})_2]^+$. In **3**, such as **2**, peak C_4 (0.1 V) is assigned to the two electron reduction of Au(III) in the $[Au(\mathbf{L3})_2Cl_2]^+$ cation and the second reduction peak, C_5 (−0.14 V), is related to the two electron reduction of Au(III) in the counter ion (Fig. 1, curve c). A comparison of curve a with curves b and c in Fig. 1 clearly confirms the presence of one (**1**) and two (**2** and **3**) Au(III) centers in the complexes with different environments.

Spectroscopy

The assignment of the IR and NMR peaks was performed according to the optimized structures of the ligands. For the numbering of the atoms see Fig. 2 and 4 (to see the spectra refer to Fig. S1–S17, ESI†).

Table 1 shows the most important vibrations in the ligands and complexes. Comparative analysis of the IR spectra of the complexes and of the free ligands revealed that the characteristic absorption bands for the stretching vibrations of –C=N– from the pyridine ring shifted towards higher frequencies in the complexes. This indicates the nitrogen atom from the pyridine ring participates in the coordination to the metal ion. The other characteristic bands of the pyridine ring of the free ligand also shifted to higher frequencies upon complexation. The bands related to the stretching vibrations of the carbonyl groups and more acidic NH groups (N3–H9 (Fig. 2), N3–H4 (Fig. 4), and N2–H5 (Fig. 4) in **L1–L3**, respectively) remained almost unchanged in the all the complexes. This fact is evidence that these groups are not involved in the complex formation. The band related to the stretching vibration of N2–H8 (Fig. 2) has disappeared in **1**, which shows the bidentate *N*-coordination of **L1** to the metal center, realized through the nitrogen atom of the pyridine ring and the deprotonated nitrogen of the hydantoin ring.[51] On the other hand, in **2** and **3**, as the nitrogen atom of the

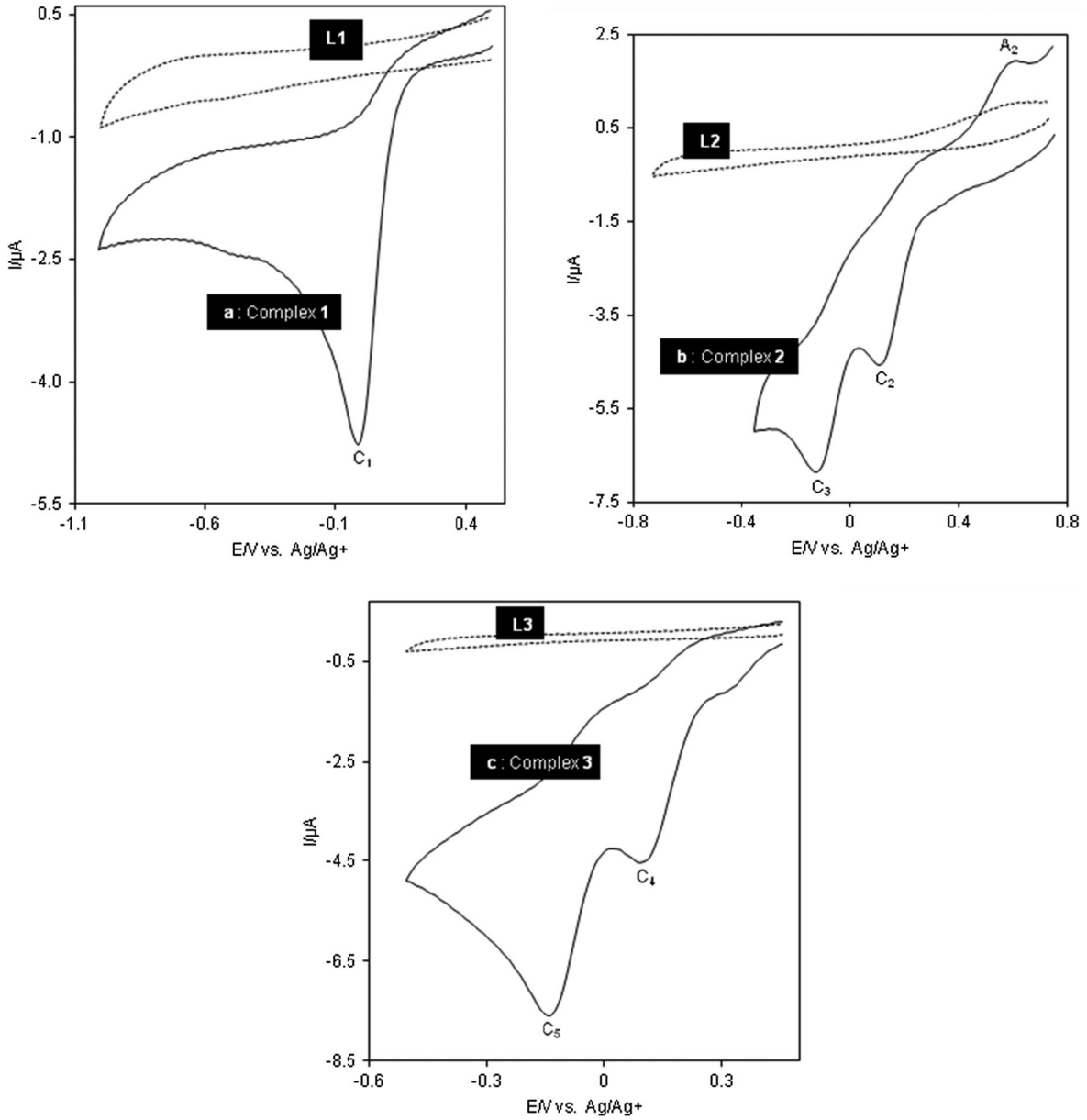

Fig. 1 Cyclic voltammograms of 1.0 mM solutions of the ligands and complexes in DMSO, containing 0.1 M tetra-*n*-butylammonium perchlorate (Bu_4NClO_4) as a supporting electrolyte, at a Pt electrode. Scan rates: 100 mV s^{-1}; t = 25 °C.

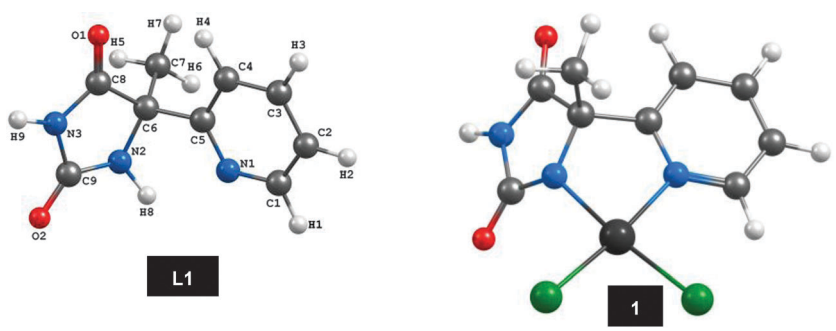

Fig. 2 Optimized structures of **L1** (left) and **1** (right) at the BP86/TZVP level of theory.

Table 1 IR selected bands (ν_{max}/cm^{-1}) of the ligands (**L1–L3**) and complexes (**1–3**), for the numbering of the atoms, see Fig. 2 and 4

Compound	$\nu_{(NH)}$	$\nu_{(CO)}$	$\nu_{(CN)}$	$\nu_{(AuCl)}$
L1	3262 (N2–H8) 3173 (N3–H9)	1759 (C8–O1) 1724 (C9–O2)	1587	—
1	— 3157	1764 1723	1604	374 and 333
L2	3244 (N2–H3) 3170 (N3–H4)	1771 (C8–O2) 1723 (C6–O1)	1594	—
2	3373 3167	1780 1720	1607	334
L3	3207 (N3–H6) 3113 (N2–H5)	1776 (C7–O1) 1729 (C8–O2)	1604	—
3	3246 3108	1780 1728	1620	374

pyridine ring only participates in the coordination, the stretching vibrations of N2–H3 (**2**) and N3–H6 (**3**) (Fig. 4) are shifted to higher frequencies. This change in the stretching frequency of these groups can be due to their proximity to the coordination site. Also, a solution IR study of the complexes in DMSO solvent supported the structures observed in the solid state, which also exist in solution. All the complexes displayed well-defined one (**2** and **3**) and two (**1**) bands in the low-energy region at 390–300 cm^{-1}, assigned to Au–Cl stretching vibrations.[53–56] These bands clearly indicate the chlorine atoms are in the *cis* and *trans* orientation, respectively.[57]

The chemical shifts from the NMR spectra of the ligands and complexes are shown in Table 2.

The ^{1}H NMR data for **1** indicates deprotonation at the NH group as the signal of N2–H8 (Fig. 2) is not visible in the spectrum. By comparing the other chemical shifts of **L1** and **1**, we can conclude the NMR data supports the participation of both the hydantoin and pyridine rings in the coordination.[51]

In the ^{1}H NMR spectra of **2** and **3**, the signals of the protons from the pyridine ring are shifted to lower frequencies compared to the spectra of the ligands. There are noticeable differences between the proton chemical shifts of the ligands and the corresponding complexes. These show that in these complexes, the most probable bonding of the ligand with the Au(III) ion is realized through the nitrogen atom of the pyridine ring. The signals for the NH groups of the hydantoin ring are slightly shifted. This fact indicates these atoms are not involved in the coordination. The impressive changes in the chemical shifts related to the carbon atoms of the pyridine ring also confirm the participation of this ring in the bonding with the metal ion. The signals of the two C=O groups from the hydantoin ring in both complexes are slightly changed. C8–O2 and C7–O1 (Fig. 4) show greater shifts toward higher frequencies than C6–O1 and C8–O2 (Fig. 4) in **2** and **3**, respectively, which could be because these groups are nearer to the coordination site. These findings are an indication that in **2** and **3**, the hydantoin ring does not participate in the coordination.

Table 2 Experimental and theoretical ^{1}H (90 and 300 MHz; DMSO; Me_4Si) and ^{13}C NMR (300 MHz; DMSO; Me_4Si) chemical shifts/ppm for the ligands and corresponding complexes, for the numbering of the atoms, see Fig. 2 and 4

	Compounds			
	L1		**1**	
	Exp.	Theo.	Exp.	Theo.
^{1}H NMR				
5,6,7-H	1.74	1.59	1.80	1.75
2-H	7.32	6.48	7.85	7.49
$J_{2,1}$	—	—	7.25	—
4-H	7.52	6.89	7.94	8.38
$J_{4,3}$	5.97	—	1.61	—
3-H	7.80	7.42	8.31	7.86
8-H	8.54	5.15	Disappeared	—
1-H	8.57	7.92	9.10	9.75
$J_{1,2}$	—	—	6.27	—
9-H	10.83	4.82	11.29	6.14
^{13}C NMR				
C-7	22.53	31.90	23.37	32.09
C-6	66.36	74.50	65.22	88.27
C-2	120.68	125.45	123.02	128.31
C-4	123.74	123.71	125.44	128.05
C-3	137.71	138.48	142.58	141.47
C-1	149.61	152.40	146.52	150.91
C-9	157.45	156.04	155.27	155.35
C-5	158.28	163.92	156.91	172.02
C-8	177.11	177.46	175.38	174.15

	Compounds			
	L2		**2**	
	Exp.	Theo.	Exp.	Theo.
^{1}H NMR				
5,6,7-H	1.69	1.64	1.76	1.83
9-H	7.39	7.31	8.13	8.62
$J_{9,8}$	7.51	—	—	—
2-H	7.88	8.24	8.71	9.37
$J_{2,9}$	7.56	—	6.54	—
8-H	8.51	8.87	8.92	7.90
1-H	8.71	9.01	8.97	4.36
3-H	8.71	4.38	9.07	8.60
4-H	—	5.89	11.16	6.32
^{13}C NMR				
C-9	25.45	30.53	25.88	30.54
C-7	63.24	72.82	62.89	74.33
C-3	123.89	125.26	127.62	151.60
C-4	133.78	136.36	139.70	154.13
C-5	136.06	140.00	139.86	151.42
C-2	147.14	154.14	142.15	131.28
C-1	149.35	149.20	143.69	141.32
C-6	157.29	153.66	156.43	153.84
C-8	177.52	176.36	175.72	153.84

	Compounds			
	L3		**3**	
	Exp.	Theo.	Exp.	Theo.
^{1}H NMR				
7,8,9-H	1.66	1.70	1.72	1.84
2-H	7.49	7.50	8.04	8.20
3-H	7.51	7.89	8.04	8.78
$J_{(2,3),(1,4)}$	4.80	—	—	—
1-H	8.58	8.68	8.91	8.75
4-H	8.59	8.69	8.91	8.57
$J_{(1,4),(2,3)}$	4.80	—	—	—
6-H	8.84	4.28	8.72	4.27
5-H	10.99	6.68	11.16	6.30

Table 2 (*continued*)

	Compounds			
	L1		**1**	
	Exp.	Theo.	Exp.	Theo.
^{13}C NMR				
C-9	25.08	31.13	25.57	30.21
C-6	63.98	76.00	64.45	73.16
C-2, C-4	120.95	122.62	123.63	130.04
C-3	148.96	150.80	151.16	164.77
C-1, C-5	150.30	152.91	144.38	152.67
C-7	156.72	162.13	156.42	153.83
C-8	176.39	178.42	175.15	172.19

Theoretical studies

Complexes Au**L1**Cl_2 (**1**), [Au(**L2**)$_2Cl_2$] (cation-**2**) and [Au(**L3**)$_2Cl_2$] (cation-**3**) exhibit square planar coordination. The optimized geometries of **L1** and **1** are shown in Fig. 2 and representative selected calculated bond parameters are listed in Table S1 (ESI†). In the case of **2** and **3**, there are two possible isomers, *cis* and *trans*. We can consider four and six conformers for *trans* and *cis* in **2**, and two and three conformers for *trans* and *cis* in **3**, respectively. Among all the optimized isomers and related conformers (see Fig. S18–S20, ESI†), only the most stable *cis* and *trans* structures are shown in Fig. 3. The calculated total energies for **2** and **3** indicate in both cases the that *trans* isomers are 24.2 and 33.4 kJ mol^{-1} more stable than the *cis* ones, respectively. Since the corresponding gold(III) complexes were obtained from 50 : 50 (v : v) ethanol–water solutions, a Conductor-like Polarizable Continuum Model (CPCM) with the dielectric constants of water or ethanol was used for further calculations. In order to compare the stability of the structures, an averaged value of the electronic energy of the complexes in water and ethanol solutions was calculated. The resulting data suggests the *trans* isomer, also in solution, is the most stable isomer in these complexes. However, the difference between the stability of the *trans* and *cis* isomers is only 15.8 and 12.9 kJ mol^{-1} for **2** and **3**, respectively. The optimized geometries of **L2**, **L3**, *trans*-**2** and *trans*-**3**

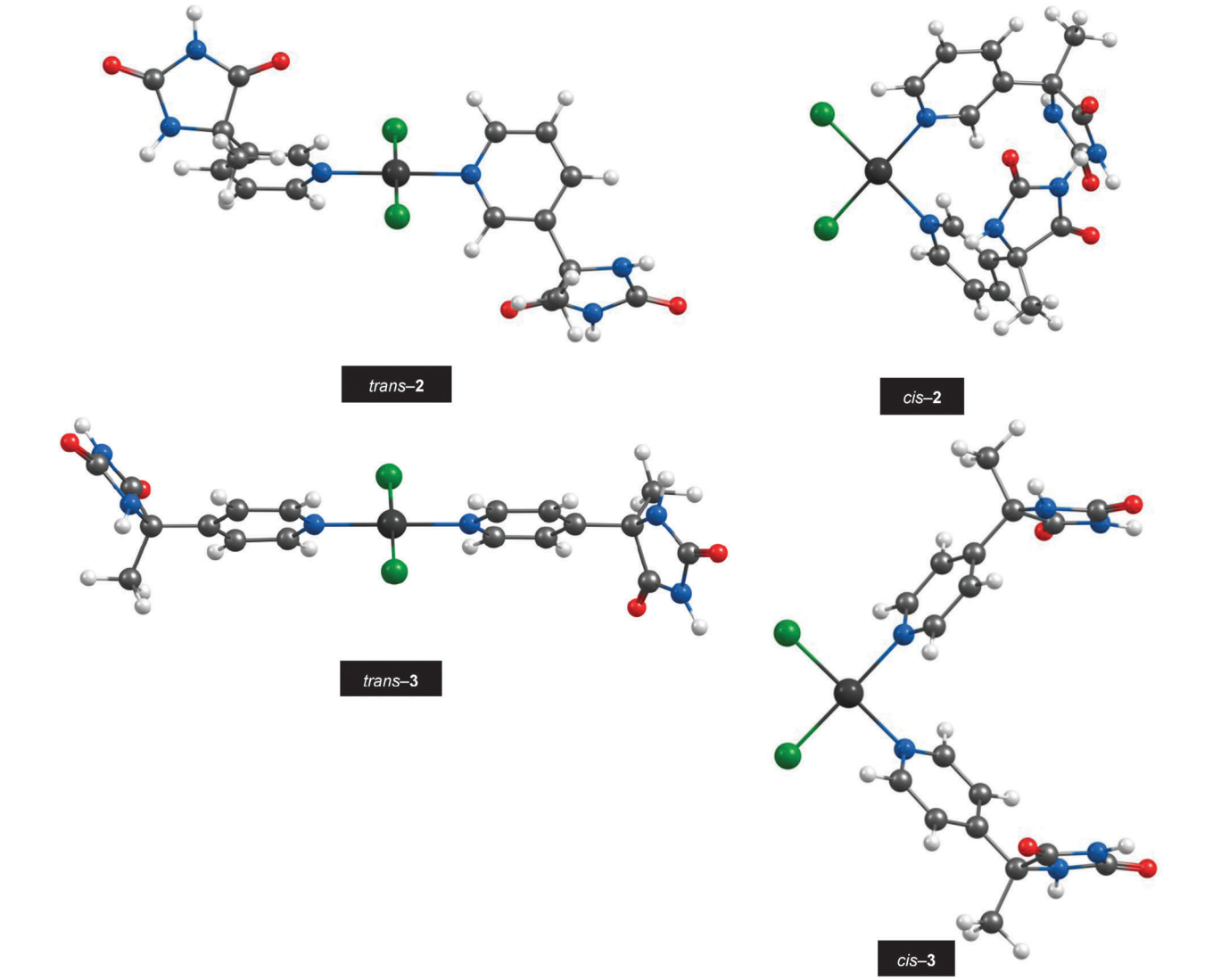

Fig. 3 The most stable *cis* and *trans* isomers of the optimized structures of **2** and **3**.

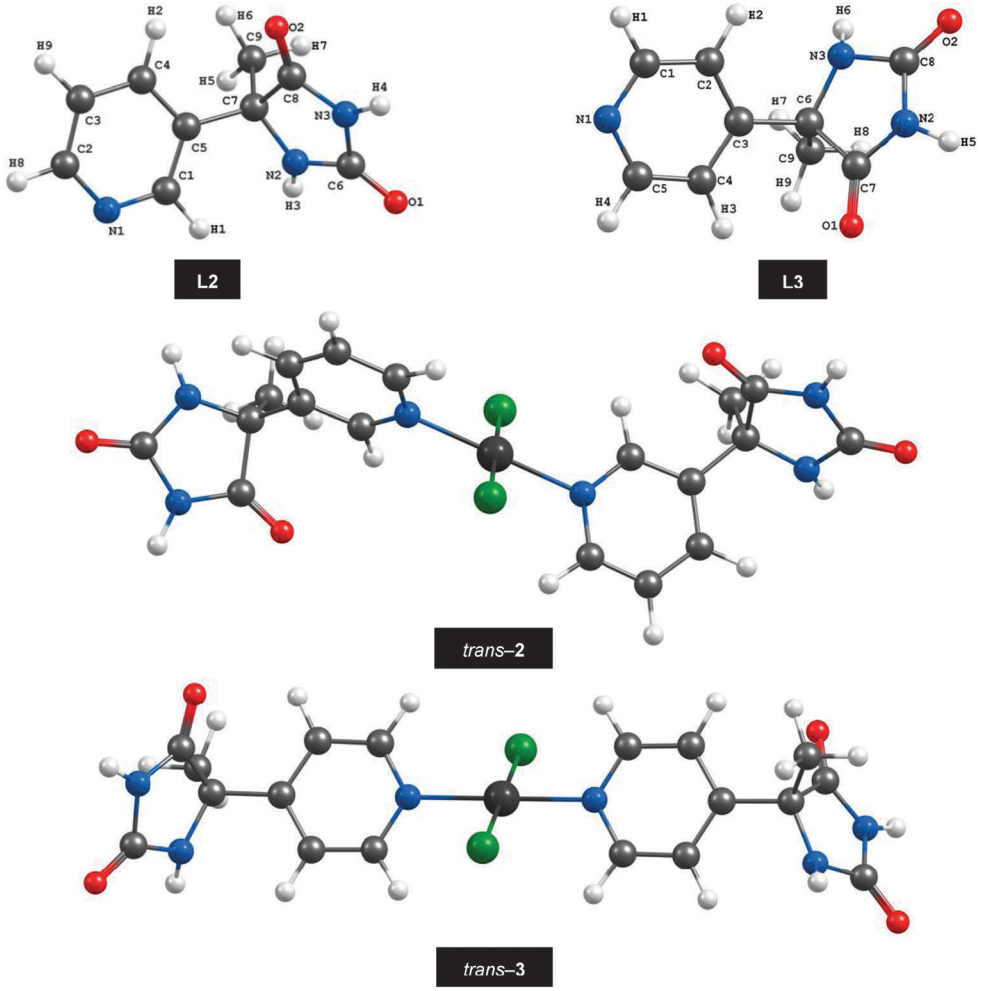

Fig. 4 Optimized structures of **L2**, **L3**, *trans*-**2**, and *trans*-**3** at the BP86/TZVP level of theory.

are shown in Fig. 4 and representative selected calculated bond parameters are listed in Tables S2 and S3 (ESI†). It should be noted that the presence of the sp^3-hybridized chiral carbon atoms (C6 in **L1** and **L3**, and C7 in **L2**) is responsible for the dihedral angle between the pyridine ring and five-membered C_3N_2 ring.

In order to consider the correlation of the ^1H and ^{13}C NMR spectra of the ligands and complexes with the calculated data obtained from their optimized structures, quantum chemical calculations of shielding constants were performed. The absolute isotropic magnetic shielding constants (σ_i) were used to obtain the chemical shifts (see eqn (1)) by referring to the standard compound tetramethylsilane (TMS) for both the H and C atoms. The TMS reference molecule was also optimized and its isotropic NMR shielding constants were calculated using the same level of theory as for the studied structures.

$$\delta_i = \sigma_{TMS} - \sigma_i \quad (1)$$

As shown in Table 2 and Fig. 5, the experimental ^1H and ^{13}C chemical shifts of all the remarkable protons, except the acidic protons (of the two –NH groups), and carbons for all the compounds are in good agreement with the calculated values. The calculated values of the acidic protons (H8 and H6 in **L1** and **1** (Fig. 2); H3 and H4 in **L2** and **2** (Fig. 4); H5 and H6 in **L3** and **3** (Fig. 4)) are unacceptable apart from the experimental values, as the continuum model has obviously not correctly described the chemical shifts associated with these protons and fails to reproduce the experimental findings for them.[58–60] However, as can be seen in Fig. 5 and Fig. S21 (ESI†), the high linear correlation coefficients (R^2) established the robustness of the assignments. Thus, it seems that the optimized and selected gas phase structures are close to the structures of these compounds in solution.

Pharmacology

Antibacterial activities. The antibacterial activity of the chemicals was studied against six bacterial strains (Table 3). All the compounds inhibited the growth of the bacterial strains, producing a zone diameter of inhibition from 8–26 mm, depending on the susceptibility of the tested bacteria. The highest antibacterial effect of **L1** was against *Escherichia coli* (13 ± 3 mm), **1** against *Staphylococcus aureus*, *Escherichia coli*, and *Proteus vulgaris* (24 ± 4 mm), **L2** and **L3** against *Staphylococcus aureus* (20 ± 3 and 20 ± 4 mm, respectively), **2** against

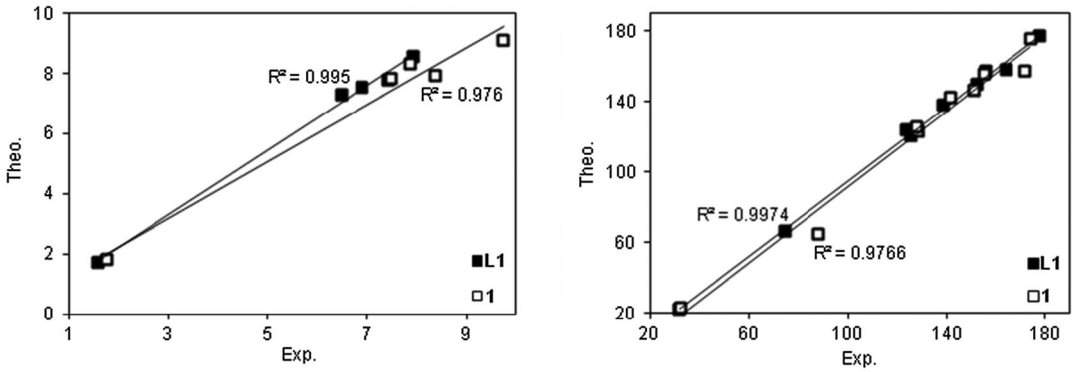

Fig. 5 Correlations between the theoretical and corresponding experimental values of the ^{1}H (the left) and ^{13}C (the right) chemical shifts (δ, ppm) for **L1** and **1** (for those of **L2**, **L3**, **2**, and **3**, see Fig. S21, ESI†).

Staphylococcus aureus (26 ± 5 mm), and **3** against *Staphylococcus aureus* and *Escherichia coli* (20 ± 4 and 20 ± 3.5 mm, respectively). Our data indicate that the highest activity of the ligands and complexes is *versus Staphylococcus aureus* and *Escherichia coli* bacteria. Based on our results, the complexes show more activity than the ligands against more microorganisms under identical experimental conditions. This would suggest that the strong chelation could facilitate the ability of a complex to cross a cell membrane and can be explained by Tweedy's chelation theory.[61] Chelation considerably reduces the polarity of the metal ion because of the partial sharing of its positive charge with donor groups and possible electron delocalization over the whole chelate ring. Such chelation can enhance the lipophilic character of the central metal atom, which subsequently favours its permeation through the lipid layer of the cell membrane.[62] On the other hand, several systems document the importance of counter ion association to charged species for drug uptake.[63] Therefore, some of the differences in the observed ligand and complex activities can be explained according to permeability improvement by counter ions in the complex system. Indeed, the $[AuCl_4]^-$ counter ion can enhance cellular uptake. As can be seen in Table 3, the minimum inhibitory concentration (MIC) of the chemicals against the tested organisms varied between 4–28 μg cm^{-3}, while those of the standard chloramphenicol changes are in the range of 1–8 μg cm^{-3}. As a result, both in terms of inhibitory potency and MIC values, the standard antibiotic chloramphenicol has stronger activity than the chemicals against these bacterial strains. Nevertheless, it is noteworthy that the inhibitory zone and MIC of complexes **1** and **2** against the *Escherichia coli* bacterium is noticeable and comparable to chloramphenicol.

***In vitro* cytotoxicity.** Cytotoxicity assay experiments were conducted to determine the effect of the Au(III) complexes on cell viability using human breast adenocarcinoma (MCF-7) and human lung carcinoma (A-549) tumor cell lines as target cells. For comparison purposes, the cytotoxicity of cisplatin, a standard antitumor drug, was evaluated under the same conditions. The concentration–response curves were drawn (Fig. 6) and the IC_{50} values were extrapolated (Table 4).

It has been proposed that gold(III) therapeutics impart tumor cytotoxicty *via* a different mechanism than cisplatin.[64] It is

Table 3 Inhibition zones (mm) and minimum inhibitory concentration (MIC) (μg cm^{-3}) of the ligands and corresponding complexes against bacterial strains

	Chemicals							
	DMSO	**L1**	**1**	**L2**	**2**	**L3**	**3**	STD[a]
Inhibition zones								
Staphylococcus aureus	—	—	24 ± 4	20 ± 3	26 ± 5	20 ± 4	20 ± 4	25 ± 3.5
Staphylococcus saprophyticus	—	—	20 ± 4	—	20 ± 3	—	16 ± 3	23 ± 5
Escherichia coli	—	13 ± 3	24 ± 4	8 ± 2	24 ± 3	—	20 ± 3.5	24 ± 4.3
Proteus vulgaris	—	—	24 ± 4	—	18 ± 3	—	13 ± 3	35 ± 8
Serratia marcescens	—	—	18 ± 3	—	14 ± 2	—	15 ± 3	22 ± 5
Bacillus cereus	—	8 ± 2	13 ± 2	10 ± 2	15 ± 3	—	15 ± 4	18 ± 2.5
MIC								
Staphylococcus aureus	—	—	4	12	4	12	6	2
Staphylococcus saprophyticus	—	—	12	—	12	—	16	4
Escherichia coli	—	16	8	20	8	—	10	8
Proteus vulgaris	—	—	16	—	20	—	28	4
Serratia marcescens	—	—	16	—	18	—	18	4
Bacillus cereus	—	28	18	24	16	—	16	1

[a] Chloramphenicol standard. Each datum represents the mean ± SE of 4–5 samples.

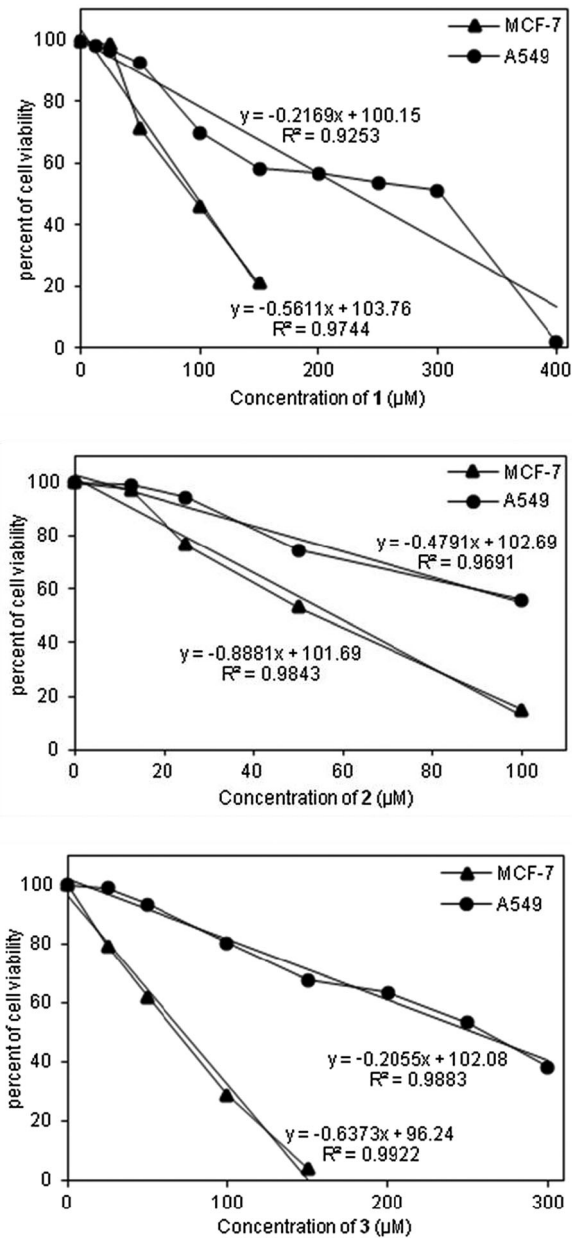

Fig. 6 Cytotoxic effects of complexes **1–3** as assessed by the MTT-dye reduction assay following 72 h treatment of MCF-7 and A-549 cells.

generally accepted that cisplatin induces tumor cell death primarily by forming coordinate covalent adducts with purine nitrogen donors in the DNA, which in turn inhibits tumor cell division and induces apoptosis.[65] Conversely, it has been reported that gold(III) compounds most likely initiate apoptosis in tumor cells through mechanisms not related to DNA binding.[64]

Evaluation of the cell viability in a panel of human tumor cell lines following a 72 h treatment revealed that the new gold(III) complexes exerted cytotoxic effects in a concentration-dependent manner. Because compounds **2** and **3** share the same anionic core and $[AuCl_4]^-$ is uniformly less active than the cationic core contained in neutral **L2** and **L3**,[7,49] the difference

Table 4 Cytotoxic activity of complexes **1–3** *vs.* cisplatin in a panel of human malignant cell lines as determined by the MTT-dye reduction assay following a 72 h continuous exposure

	IC_{50} value[a] (μM)			
Cell lines	**1**	**2**	**3**	Cisplatin
MCF-7[b]	95.03 ± 9.09	57.88 ± 4.71	72.49 ± 4.41	20.99 ± 3.60
A-549[c]	225.08 ± 16.89	107.74 ± 12.86	234.53 ± 9.44	11.73 ± 2.96

[a] Means ± sd of 8 separate wells, run in triplicate. [b] Breast adenocarcinoma. [c] Lung carcinoma.

in the activity of these complexes can be attributed to the difference in the structure and coordination mode of the ligands in the cationic core and is comparable to the neutral complex **1** containing deprotonated **L1**. It should be noted that, undoubtedly, the counter ion in **2** and **3** is important to the properties and potential processing that might take place under physiological conditions, as previously mentioned. The IC_{50} values (Table 4) of the three complexes are approximately 2–5 and 9–20 times higher than that of cisplatin against MCF-7 and A549 cell lines, respectively. As can be seen, the most profound effect of these complexes is against MCF-7 cell lines, making them (especially **2**) promising for further pharmacological evaluation. Although these complexes are far less active against A549 cell lines compared to the referent agent cisplatin, when they are applied at high micromolar concentrations, they will exhibit significant inhibiting activity, causing almost total eradication of malignant cells. The results of the above studies provide another challenge to the paradigm that square planar complexes in a *trans* conformation do not show any biological activity. They are in accord with existing data, which suggests that it should be possible to confer cytotoxicity to *trans*-configuration compounds by introducing bulky spectator ligands,[66,67] such as those used here, which increase the stability of the gold(III) state towards redox reactions.

Conclusions

The present study describes the synthesis and characterization of new Au(III) complexes, **1–3**, of 5-methyl-5(pyridyl)-2,4-imidazolidenedione ligands, **L1–L3**. Physico-chemical and spectroscopic data showed the ligands exhibit bidentate (**L1**) and monodentate (**L2** and **L3**) *N*-coordination to the metal center. Based on the experimental results, the complexes have a square planar structure with 1 : 1 (**1**) and 2 : 1 (**2** and **3**) ligand–metal ratios. In **2** and **3**, $[AuCl_4]^-$ acts as a counter-ion. DFT calculations support the formation of *trans* isomers for complexes **2** and **3**.

The results from the antibacterial studies demonstrate the chemicals have lower activity against the tested bacterial strains, except for the *Escherichia coli* bacterium, than chloramphenicol. The *in vitro* cytotoxicity of the complexes against breast cancer MCF-7 and lung cancer A-549 cell lines indicates the gold(III) complexes exhibit relevant cytotoxic properties, especially when tested on breast cancer cells. Among the complexes, **2** shows comparable cytotoxicity profiles to that of

cisplatin and seems to be a good candidate for future pharmacological evaluation. The results of the above studies provide another challenge to the paradigm that square planar complexes in a *trans* conformation do not show any biological activity.

Experimental

Materials and physical measurements

All the necessary chemicals obtained from commercial suppliers were reagent grade and used without further purification. The gold content was recorded by a Perkin-Elmer ICP-MS spectrometer performed on a wear metal analyzer 400. The carbon, nitrogen and hydrogen contents were determined by elemental analysis carried out on a 'Vario EL III' elemental analyzer. IR spectra were recorded on a Perkin-Elmer and Bruker vertex 70 FT-IR spectrophotometer in the range of 4000–400 and 400–150 cm^{-1} as KBr and ATR cells, respectively. NMR spectra were obtained on 90 MHz Jeol and 300 MHz Bruker spectrometers in DMSO-d_6 as the solvent. Melting points were determined using a SMP_3 apparatus. The molar conductivity of the complexes in DMSO was measured by means of a Metrohm conductometer 712.

Electrochemical studies

Cyclic voltammetric experiments were carried out using an Autolab model PGSTAT 20 potentiostat/galvanostat. The data were recorded using a Pt disc (2.2 mm diameter), a platinum counter electrode, and an Ag/Ag^+ reference electrode (all the electrodes were from AZAR Electrodes). A DMSO solution (containing tetra-*n*-butylammonium perchlorate, 0.1 M, as a supporting electrolyte, the ligands and complexes, 1.0 mM) was placed in a single compartment electrochemical cell and degassed by bubbling with DMSO saturated with N_2(g). The N_2 atmosphere was continuously maintained above the solution while the experiments were in progress.

Computational details

The geometries of **L1–L3** and the corresponding Au(III) complexes in the gas phase were fully optimized using the BP86 functional.[68,69] The def2-TZVP[70] basis set was employed for all the atoms and the structures were optimized without symmetry restrictions. All the calculations were performed using the Gaussian 03 set of programs.[71] The Conductor-like Polarizable Continuum Model (CPCM),[72] as implemented in Gaussian 03, was used for the prediction of the solvent influence on the relative stability of the complexes. The ^1H and ^{13}C NMR shielding results were obtained at the same level of theory. The ^1H and ^{13}C isotropic shielding constants were calculated using the gauge independent atomic orbital (GIAO) method.[73,74]

Antibacterial study

Test organisms. Standard strains of the following microorganisms were used as test organisms: *Staphylococcus aureus* (ATCC 6633), *Staphylococcus saprophyticus* (ATCC 15305), *Escherichia coli* (Lio), *Proteus vulgaris* (Lio), *Serratia marcescens* (PTCC 1330), and *Bacillus cereus* (ATCC 7064). Some microorganisms were obtained from Persian Type Culture Collection, Tehran, Iran and others were locally isolated (Lio). The organisms were sub-cultured in a nutrient broth and nutrient agar (Oxiod Ltd.) for use in the experiments, while diagnostic sensitivity test agar (DST) (Oxoid Ltd.) was used in the antibiotic sensitivity testing.

Sensitivity testing. For the bioassays, a suspension of approximately 1.5×10^8 cells per cm^3 in sterile normal saline was prepared, as described by Forbes *et al.*[75] The sensitivity testing was determined using the agar-well diffusion method.[76] In each disk, 30 μ dm^3 of the chemicals were loaded. The bacterial isolates were first grown in a nutrient broth for 18 h before use. The inoculum suspensions were standardized and then tested against the effect of the chemicals at amounts of 30 μ dm^3 for each disk in a DST medium. The plates were later incubated at 37 ± 0.5 °C for 24 h, after which they were evaluated for zones of inhibition, an area of media where bacteria are unable to grow due to the presence of a drug that impedes their growth. The effects were compared with that of the standard antibiotic chloramphenicol at a concentration of 1 mg cm^{-3}.[77] The minimum inhibitory concentration (MIC) of the chemicals was determined by tube dilution techniques in a Mueller–Hinton broth (Merck) according to NCCLS.[78] The experiments were repeated at least three to five times for each organism and the data are presented as the mean ± SE of 3–5 samples.

Cytotoxicity assay

Cell lines and culture conditions. The following cell lines were prepared from the Iranian Biological Resource Center and used in the experiments: MCF-7 (DSMZ No.: ACC 115, cell type: human estrogen receptor positive breast adenocarcinoma, established from the pleural effusion of a 69-year-old Caucasian woman with metastatic mammary carcinoma); A-549 (DSMZ No.: ACC 107, cell type: human lung carcinoma, established from an explanted lung tumor which was removed from a 58-year-old Caucasian man); the cells were used to induce tumors in athmyic mice and to synthesize lecithin. MCF-7 and A549 cells were grown as monolayer adherent cultures in 90% DMEM supplemented with 10% FBS. 2×10^4 cells per well cultured in 96 well plates. All the cell lines were maintained in tissue culture flasks in a humidified atmosphere at 37 °C and 5% CO_2. The cells were kept in log phase by supplementation with a fresh medium 2–3 times per week. Adherent cells were reset by trypsinization twice weekly.

Cytotoxicity assessment. The cytotoxicity of the complexes was assessed using the MTT [3-(4,5-dimethylthiazol-2-yl)-2,5-diphenyltetrazolium bromide] dye reduction assay[79] with some modifications.[80] Exponentially growing cells were seeded in 96-well microplates (100 μdm^3 per well at a density of 2×10^5 cells per cm^3) and allowed to grow for 24 h prior to exposure to the studied compounds. Stock solutions of the complexes were freshly prepared in DMSO and then diluted with a corresponding growth medium. At the final dilutions, the solvent concentration never exceeded 0.5%. The cells were exposed to the test agents for 72 h, whereby for each concentration, a set of 8 separate wells were used. After incubation with

the test compounds, MTT solution (5 mg cm^{-3} in PBS) aliquots were added to each well. The plates were further incubated for 4 h at 37 °C and the formazan crystals formed were dissolved by adding 100 μ dm^3 per well of DMSO. Absorption of the samples was measured by an ELISA reader (Uniscan Titertec) at 570 nm. The survival fraction was calculated as a percentage of the untreated control.

Data processing and statistics. The cytotoxicity data were processed using commercially available software packages (Microsoft Excel and GraphPad Prizm for PC). The MTT survival plots were fitted to sigmoidal dose–response curves and the corresponding IC_{50} values were calculated on the basis of 8 separate wells, run in triplicate. The statistical procedures included Student's *t*-test with $p \leq 0.05$ set as the significance level.

Synthesis and characterization

Synthesis of the ligands. The ligands were prepared by a previously published method.[81] Since in the original work these compounds were poorly characterized, and also for comparative purposes, spectroscopic characterization was performed.

Synthesis of the complexes. $H[AuCl_4]\cdot xH_2O$ in 3 cm^3 water (0.3397 g, 1.000 mmol) was added to a solution of the ligand (0.1911 g, 1.000 mmol) in 3 cm^3 water–ethanol 50% and the resulting solution was stirred at room temperature for 24 h. The solid product was precipitated from the reaction mixture. The stable complex was filtered off, washed with cold water and dried under vacuum. The purity was checked by thin layer chromatography with $CH_3COOC_2H_5$–C_2H_5OH = 2 : 1as the eluent. The substance is soluble in DMSO.

*Dichloro-(5-methyl-5-(2-pyridyl)-2,4-imidazolidenatedione)gold(III) (**1**).* (0.3997 g, 87.2%). MP 224 °C. Found: C, 23.97; H, 1.50; N, 9.22; Au, 43.40. Calc. for $AuCl_2C_9H_8N_3O_2$: C, 23.60; H, 1.76; N, 9.17; Au, 43.00. Λ_M (10^{-3} M, DMSO) 11.70 Ω^{-1} cm^2 mol^{-1}.

trans-Dichloro-bis(5-methyl-5-(3-pyridyl)-2,4-imidazolidenedione)-gold(III) tetrachloroaurate(III) (**2**). (0.4581 g, 92.6%). MP 258 °C. Found: C, 22.14; H, 1.66; N, 8.58; Au, 39.50. Calc. for $Au_2Cl_6C_{18}H_{18}N_6O_4$: C, 21.86; H, 1.83; N, 8.50; Au, 39.83. Λ_M (10^{-3} M, DMSO) 79.12 Ω^{-1} cm^2 mol^{-1}.

trans-Dichloro-bis(5-methyl-5-(4-pyridyl)-2,4-imidazolidenedione)-gold(III) tetrachloroaurate(III) (**3**). (0.4457 g, 90.1%). MP 227 °C. Found: C, 22.21; H, 1.94; N, 8.59; Au, 39.42. Calc. for $Au_2Cl_6C_{18}H_{18}N_6O_4$: C, 21.86; H, 1.83; N, 8.50; Au, 39.83. Λ_M (10^{-3} M, DMSO) 43.45 Ω^{-1} cm^2 mol^{-1}.

Acknowledgements

We are grateful to Bu-Ali Sina University for financial support.

Notes and references

1 L. Messori and G. Marcon, *Met. Ions Biol. Syst.*, 2004, **42**, 385–424.
2 L. Messori, G. Marcon and P. Orioli, *Bioinorg. Chem. Appl.*, 2003, **1**, 177–187.
3 C. X. Zhang and S. J. Lippard, *Curr. Opin. Chem. Biol.*, 2003, **7**, 481–489.
4 G. Marcon, S. Carotti, M. Coronnello, L. Messori, E. Mini, P. Orioli, T. Mazzei, M. A. Cinellu and G. Minghetti, *J. Med. Chem.*, 2002, **45**, 1672–1677.
5 E. R. Tiekink, *Gold Bull.*, 2003, **36**, 117–124.
6 C. F. Shaw III, *Chem. Rev.*, 1999, **99**, 2589–2600.
7 E. R. Tiekink, *Crit. Rev. Oncol. Hematol.*, 2002, **42**, 225–248.
8 M. Coronnello, G. Marcon, S. Carotti, B. Caciagli, E. Mini, T. Mazzei, P. Orioli and L. Messori, *Oncol. Res.*, 2001, **12**, 9–10.
9 L. Messori, P. Orioli, C. Tempi and G. Marcon, *Biochem. Biophys. Res. Commun.*, 2001, **281**, 352–360.
10 G. Marcon, L. Messori and P. Orioli, *Expert Rev. Anti-Infect. Ther.*, 2002, **2**, 337–346.
11 L. Messori, F. Abbate, G. Marcon, P. Orioli, M. Fontani, E. Mini, T. Mazzei, S. Carotti, T. O'Connell and P. Zanello, *J. Med. Chem.*, 2000, **43**, 3541–3548.
12 F. Abbate, P. Orioli, B. Bruni, G. Marcon and L. Messori, *Inorg. Chim. Acta*, 2000, **311**, 1–5.
13 P. Calamai, A. Guerri, L. Messori, P. Orioli and G. Paolo Speroni, *Inorg. Chim. Acta*, 1999, **285**, 309–312.
14 P. Calamai, S. Carotti, A. Guerri, L. Messori, E. Mini, P. Orioli and G. Paolo Speroni, *J. Inorg. Biochem.*, 1997, **66**, 103–109.
15 R. G. Buckley, A. M. Elsome, S. P. Fricker, G. R. Henderson, B. R. Theobald, R. V. Parish, B. P. Howe and L. R. Kelland, *J. Med. Chem.*, 1996, **39**, 5208–5214.
16 P. Calamai, S. Carotti, A. Guerri, T. Mazzei, L. Messori, E. Mini, P. Orioli and G. P. Speroni, *Anti-Cancer Drug Des.*, 1998, **13**, 67–80.
17 F. Cossu, Z. Matovic, D. Radanovic and G. Ponticelli, *Farmaco*, 1994, **49**, 301–302.
18 J. N. Carrasco, J. J. Criado, R. O. I. Macías, J. L. Manzano, J. J. Marín, M. Medarde and E. Rodríguez, *J. Inorg. Biochem.*, 2001, **84**, 287–292.
19 J. A. Cuadrado, W. X. Zhang, W. Hang and V. Majidi, *J. Environ. Monit.*, 2000, **2**, 355–359.
20 S. Carotti, G. Marcon, M. Marussich, T. Mazzei, L. Messori, E. Mini and P. Orioli, *Chem.-Biol. Interact.*, 2000, **125**, 29–38.
21 R. Parish, *Met.-Based Drugs*, 1999, **6**, 271–276.
22 F. Zamora, E. Zangrando, M. Furlan, L. Randaccio and B. Lippert, *J. Organomet. Chem.*, 1998, **552**, 127–134.
23 A. Moustatih and A. Garnier-Suillerot, *J. Med. Chem.*, 1989, **32**, 1426–1431.
24 M.-T. Lee, T. Ahmed and M. E. Friedman, *J. Enzyme Inhib. Med. Chem.*, 1989, **3**, 23–33.
25 F. Van Valen, H. Franck, H. Krüskemper and E. Keck, *Biochem. Biophys. Res. Commun.*, 1985, **130**, 580–587.
26 E. Keck, F. van Valen and H. Zeidler, *Z. Rheumatol.*, 1986, 304–309.
27 N. Hadjiliadis, G. Pneumatikakis and R. Basosi, *J. Inorg. Biochem.*, 1981, **14**, 115–126.
28 A. A. Isab and P. J. Sadler, *Biochim. Biophys. Acta, Protein Struct.*, 1977, **492**, 322–330.
29 D. Chatterji, U. Nandi and S. Podder, *Biopolymers*, 1977, **16**, 1863–1878.

30 P. Brown, *Proc. R. Soc. Med.*, 1977, **70**, 41–43.
31 D. W. Gibson, M. Beer and R. J. Barrnett, *Biochemistry*, 1971, **10**, 3669–3679.
32 M. B. Dinger and W. Henderson, *J. Organomet. Chem.*, 1998, **560**, 233–243.
33 W. Henderson, *J. Organomet. Chem.*, 1998, **557**, 231–241.
34 E. C. Constable, R. P. G. Henney and T. A. Leese, *J. Organomet. Chem.*, 1989, **361**, 277–282.
35 J. Vicente, M. D. Bermúdez and F. J. Carrión, *Inorg. Chim. Acta*, 1994, **220**, 1–3.
36 M. Nonoyama, K. Nakajima and K. Nonoyama, *Polyhedron*, 1997, **16**, 4039–4044.
37 K. Ortner and U. Abram, *Inorg. Chem. Commun.*, 1998, **1**, 251–253.
38 M. B. Dinger, W. Henderson, B. K. Nicholson and W. T. Robinson, *J. Organomet. Chem.*, 1998, **560**, 169–181.
39 H. Ieda, H. Fujiwara and Y. Fuchita, *Inorg. Chim. Acta*, 2001, **319**, 203–206.
40 Y. Fuchita, H. Ieda, S. Wada, S. Kameda and M. Mikuriya, *J. Chem. Soc., Dalton Trans.*, 1999, 4431–4435.
41 M. Nonoyama and K. Nakajima, *Transition Met. Chem.*, 1999, **24**, 449–453.
42 A. Ericson, J. C. Arthur, R. S. Coleman, L. I. Elding and S. K. Elmroth, *J. Chem. Soc., Dalton Trans.*, 1998, 1687–1692.
43 B. Pitteri and M. Bortoluzzi, *Transition Met. Chem.*, 2006, **31**, 1028–1033.
44 A. Vujačić, J. Savić, S. Sovilj, K. Mészáros Szécsényi, N. Todorović, M. Ž. Petković and V. Vasić, *Polyhedron*, 2009, **28**, 593–599.
45 B. Pitteri, M. Bortoluzzi and V. Bertolasi, *Transition Met. Chem.*, 2008, **33**, 649–654.
46 C. A. Lopez and G. G. Trigo, *Adv. Heterocycl. Chem.*, 1985, **38**, 177–228.
47 A. Camerman and N. Camerman, *Acta Crystallogr., Sect. B: Struct. Crystallogr. Cryst. Chem.*, 1971, **27**, 2205–2211.
48 T. V. Segapelo, I. A. Guzei, L. C. Spencer, W. E. V. Zyl and J. Darkwa, *Inorg. Chim. Acta*, 2009, **362**, 3314–3324.
49 P. Shi, Q. Jiang, J. Lin, Y. Zhao, L. Lin and Z. Guo, *J. Inorg. Biochem.*, 2006, **100**, 939–945.
50 W. J. Geary, *Coord. Chem. Rev.*, 1971, **7**, 81–122.
51 S. J. Sabounchei, P. Shahriary, Y. Gholiee, S. Salehzadeh, H. R. Khavasi and A. Chehregani, *Inorg. Chim. Acta*, 2014, **409**, 265–275.
52 U. Koelle and A. Laguna, *Inorg. Chim. Acta*, 1999, **290**, 44–50.
53 K. Palanichamy and A. C. Ontko, *Inorg. Chim. Acta*, 2006, **359**, 44–52.
54 M. A. Cinellu, F. Cocco, G. Minghetti, S. Stoccoro, A. Zucca and M. Manassero, *J. Organomet. Chem.*, 2009, **694**, 2949–2955.
55 J. S. Casas, M. V. Castaño, M. C. Cifuentes, J. C. García-Monteagudo, A. Sanchez, J. Sordo and U. Abram, *J. Inorg. Biochem.*, 2004, **98**, 1009–1016.
56 A. McConnell, D. Brown and W. Smith, *Spectrochim. Acta, Part A*, 1981, **37**, 583–585.
57 K. Nakamoto, *Infrared and Raman Spectra of Inorganic and Coordination Compounds: Theory and Applications in Inorganic Chemistry*, John Wiley, The University of Michigan, 1997.
58 V. Chiş, A. Pîrnău, M. Vasilescu, R. A. Varga and O. Oniga, *THEOCHEM*, 2008, **851**, 63–74.
59 N. T. Abdel Ghani and A. M. Mansour, *Spectrochim. Acta, Part A*, 2012, **86**, 605–613.
60 N. T. A. Ghani and A. M. Mansour, *Spectrochim. Acta, Part A*, 2011, **81**, 754–763.
61 B. G. Tweedy, *Phytopathalogy*, 1964, **55**, 910–914.
62 M. Tümer, D. Ekinci, F. Tümer and A. Bulut, *Spectrochim. Acta, Part A*, 2007, **67**, 916–929.
63 A. Chatkon, P. B. Chatterjee, M. A. Sedgwick, K. J. Haller and D. C. Crans, *Eur. J. Inorg. Chem.*, 2013, 1859–1868.
64 A. N. Wein, A. T. Stockhausen, K. I. Hardcastle, M. R. Saadein, S. B. Peng, D. Wang, D. M. Shin, Z. G. Chen and J. F. Eichler, *J. Inorg. Biochem.*, 2011, **105**, 663–668.
65 M. Gielen and E. R. T. Tiekink, *Metallotherapeutic Drugs and Metal-Based Diagnostic Agents: The Use of Metals in Medicine*, Wiley, 2005.
66 G. Momekov, A. Bakalova and M. Karaivanova, *Curr. Med. Chem.*, 2005, **12**, 2177–2191.
67 A. Bakalova, H. Varbanov, R. Buyukliev, G. Momekov, D. Ferdinandov, S. Konstantinov and D. Ivanov, *Eur. J. Med. Chem.*, 2008, **43**, 958–965.
68 A. D. Becke, *Phys. Rev. A: At., Mol., Opt. Phys.*, 1988, **38**, 3098–3100.
69 J. P. Perdew, *Phys. Rev. B*, 1986, **33**, 8822–8824.
70 F. Weigend and R. Ahlrichs, *Phys. Chem. Chem. Phys.*, 2005, **7**, 3297–3305.
71 M. J. Frisch, G. W. Trucks, H. B. Schlegel, G. E. Scuseria, M. A. Robb, J. R. Cheeseman, J. A. J. Montgomery, T. Vreven, K. N. Kudin, J. C. Burant, J. M. Millam, S. S. Iyengar, J. Tomasi, V. Barone, B. Mennucci, M. Cossi, G. Scalmani, N. Rega, G. A. Petersson, H. Nakatsuji, M. Hada, M. Ehara, K. Toyota, R. Fukuda, J. Hasegawa, M. Ishida, T. Nakajima, Y. Honda, O. Kitao, H. Nakai, M. Klene, X. Li, J. E. Knox, H. P. Hratchian, J. B. Cross, C. Adamo, J. Jaramillo, R. Gomperts, R. E. Stratmann, O. Yazyev, A. J. Austin, R. Cammi, C. Pomelli, J. W. Ochterski, P. Y. Ayala, K. Morokuma, G. A. Voth, P. Salvador, J. J. Dannenberg, V. G. Zakrzewski, S. Dapprich, A. D. Daniels, M. C. Strain, O. Farkas, D. K. Malick, A. D. Rabuck, K. Raghavachari, J. B. Foresman, J. V. Ortiz, Q. Cui, A. G. Baboul, S. Clifford, J. Cioslowski, B. B. Stefanov, G. Liu, A. Liashenko, P. Piskorz, I. Komaromi, R. L. Martin, D. J. Fox, T. Keith, M. A. Al-Laham, C. Y. Peng, A. Nanayakkara, M. Challacombe, P. M. W. Gill, B. Johnson, W. Chen, M. W. Wong, C. Gonzalez and J. A. Pople, *Gaussian*, Gaussian, Inc., Pittsburgh, PA, 2003.
72 V. Barone and M. Cossi, *J. Phys. Chem. A*, 1998, **102**, 1995–2001.
73 K. Wolinski, J. F. Hinton and P. Pulay, *J. Am. Chem. Soc.*, 1990, **112**, 8251–8260.
74 G. Magyarfalvi and P. Pulay, *J. Chem. Phys.*, 2003, **119**, 1350–1358.

75 A. A. Forbes, D. F. Sahm, A. S. Weissfeld and E. A. Trevino, *Method for Testing Antimicrobial Effectiveness in Diagnostic Microbiology*, Bailey & Scott's, The University of Michigan, 1990.
76 A. D. Russel and J. R. Furr, *J. Appl. Bacteriol.*, 1977, **43**, 23–25.
77 M. Khan and A. Omoloso, *Fitoterapia*, 2003, **74**, 695–698.
78 N. C. f. C. L. Standards, Wayne, PA, 2008.
79 T. Mosmann, *J. Immunol. Methods*, 1983, **65**, 55–63.
80 I. Judson, M. McKeage, J. Hanwell, C. Berry, P. Mistry, F. Raymond, G. Poon, B. Murrer and K. Harrap, *Platinum and Other Metal Coordination Complexes in Cancer Chemotherapy: The Clinical Development of the Oral Platinum Anticancer Agent JM216*, H. M. Press, New York, 1996.
81 C. C. Chu and P. Teague, *J. Org. Chem.*, 1958, **23**, 1578.

